An experimental study on the development of fracture process in plain concrete beams using *b*-value analysis of AE signals

B. K. Raghu Prasad & R. Vidya Sagar
Department of Civil Engineering, Indian Institute of Science, Bangalore, India

ABSTRACT: An attempt has been made to study experimentally the fracture process in plain concrete beams using b-value analysis of Acoustic Emission (AE) signals. It is well known that stress waves released during the fracture process in materials are known as acoustic emissions. We carried out three point bend tests on plain concrete beams and AE produced during the fracture of notched three point bend (TPB) plain concrete beam specimens have been used to compute the b-values. The b-value based on Gutenberg-Richter formula is calculated from the frequency-amplitude plots for incremental ranges of the monotonically applied load, while in literature the same is studied under cyclic loading. The concrete specimens were tested by Material Testing System (MTS) of 1200kN capacity by Crack Mouth Opening Displacement (CMOD) control at the rate of 0.0004mm/sec following RILEM - Réunion Internationale des Laboratoires d'Essais et de Recherches sur les Matériaux et les Constructions (The International Union of Testing and Research Laboratories for Materials and Structures) recommendations. The 28-day compressive strengths of concrete cubes were 77.9 MPa, 63.7 MPa and 60.5 MPa. The observations done in the present experimental study have some important applications for monitoring the integrity of structures.

1 INTRODUCTION

In general concrete is a highly heterogeneous, quasi-brittle and composite material. The nature of concrete fracture behavior continues to be the subject of intensive research[1-4]. Excessive use, overloading, climatic conditions and lack of sufficient maintenance are some causes of deterioration of civil engineering structures. Civil engineering structures incorporate complicated multi-material components that require periodic structural monitoring. In general the civil engineering structural components require sophisticated non-destructive tests which must be drawn from a range of physical phenomena[5-6]. It is well known that Non-destructive testing (NDT) and non-destructive evaluation (NDE) techniques are methods for probing inside the materials[5-6]. Non-destructive testing and evaluation methods gather important material or structural conditions in situ through non-destructive phenomenon. It is observed that many civil engineering structures are approaching the limit of their service life[7]. AE technique is one of the most sensitive techniques to non-invasively monitor deformation, fatigue and fracture of materials including concrete. For more than four decades AE technique is being used in civil engineering practice and AE technique is well suited for monitoring fracture process[5-7]. In general two types of structural monitoring processes using AE technique are possible. One is global monitoring of the complete structure which is intended to yield general information on the whole structure[8,30]. The second one is local monitoring of the structure which yields a more detailed understanding of a certain area of a beam or bridge or liquid storage tank or any other structure[8,9,30]. The classic sources of acoustic emissions are defect-related deformation processes such as crack growth and plastic deformation[8]. AE is caused due to localized and rapid release of strain energy in a stressed material. AE is a class of phenomena whereby transient elastic waves are generated by rapid release of energy from a localized sources within a material, or the transient waves so generated[5]. AE energy causes stress waves to propagate through the specimen. These stress waves can be detected on the specimen surface and analyzed to deduce the magnitude and nature of the damage present in materials[5,8]. Among various AE parameters, the most significant one is *b*-value which is derived from the amplitude distribution data of AE following the methods used in seismology. When studying the highly heterogeneous materials like concrete subjected to constant or increasing stress experimental tests provide a typical power-law relation between the amplitude of AE events and their frequency[13-19]. Similar analyses are commonly

employed at different scales in seismology where it was proved that a larger number of earthquakes have smaller magnitude and a few earthquakes have higher magnitude. Fracture is a failure process by which new surfaces in the form of crack are formed in a material or existing crack surfaces are extended[1-4]. Various conditions and stages of fracture can be visualized, namely crack initialization, fracture initiation, fracture propagation, stable fracture and unstable fracture[1-4]. The type of crack generated during the fracture process of AE signals with varying frequency ranges and amplitudes. The differences in frequency ranges of AE signals and amplitudes can be related to the damage occurred in the structure. In seismology and rock mechanics the analysis of b-value is a well-known concept[20-25]. Fracture mechanics along with AE technique can be used to evaluate safety of structures. The b-value analysis has been carried out on a reinforced concrete beam tested under cyclic loading in the laboratory[20]. The study concluded that the minimum b-value suggests the formation of microcracks while the maximum b-value trend employs microcrack growth[20]. The b-value analysis and improved b-value analysis were studied using the AE produced during the uniaxial compression tests on Godhra granites[25,29]. The trend of b-value versus time was studied in rock fracture and it was concluded that a single minimum b-value was observed just before dynamic fracture takes place[28]. Using acoustic emission technique the damage in concrete and masonry was studied using fracture mechanics criteria[27]. The improved b-value analysis of AE signals was applied to study the fracture process in concrete[29]. The research done so far related to application of b-value analysis to structural concrete in civil engineering is meager[20]. In this experimental study it is intended to study the b-value analysis of AE connected to concrete fracture.

2 FREQUENCY-MAGNITUDE RELATIONSHIP

It is well know from seismology that events of bigger magnitude occur less repeatedly than events of minor magnitude[13-19]. This corresponds to the well-known Guttengberg-Richter relationship between frequency and magnitude[13-19].

$$\log_{10} N(M) = a - bM \qquad (1)$$

Where M is earthquake magnitude and $N(M)$ is the number of earthquakes of a given magnitude M. "a" and "b" are constants[13-19]. From equation (1) the b-value is the negative gradient of the log-linear plot of earthquake frequency-magnitude and hence (1) represents the slope of the amplitude distribution[13-19]. The Guttengberg-Richter relation for frequency

versus magnitude can be applied to the AE method to study the scaling of the amplitude distribution of the acoustic emission waves generated during the cracking process in the test specimen at laboratory or in engineering structures. Studies have noted a power law frequency-magnitude relationship for AE events[23-24]. The AE amplitude is considered as the largest voltage peak in the AE signal wave and customarily expressed in decibels[5] and AE amplitude is associated with the magnitude of the fracture. The b-value changes systematically with the different stages of fracture growth[24,27,28]. Therefore the b-value could be used to study the development of fracture process taking place in the test sample or structure[20]

3 EXPERIMENTAL INVESTIGATION

3.1 *Experimental setup*

The data presented in this experimental study refer to the experiments carried out on TPB specimens with different strength. Figure 1a shows the experimental setup with the instrumented test specimen.
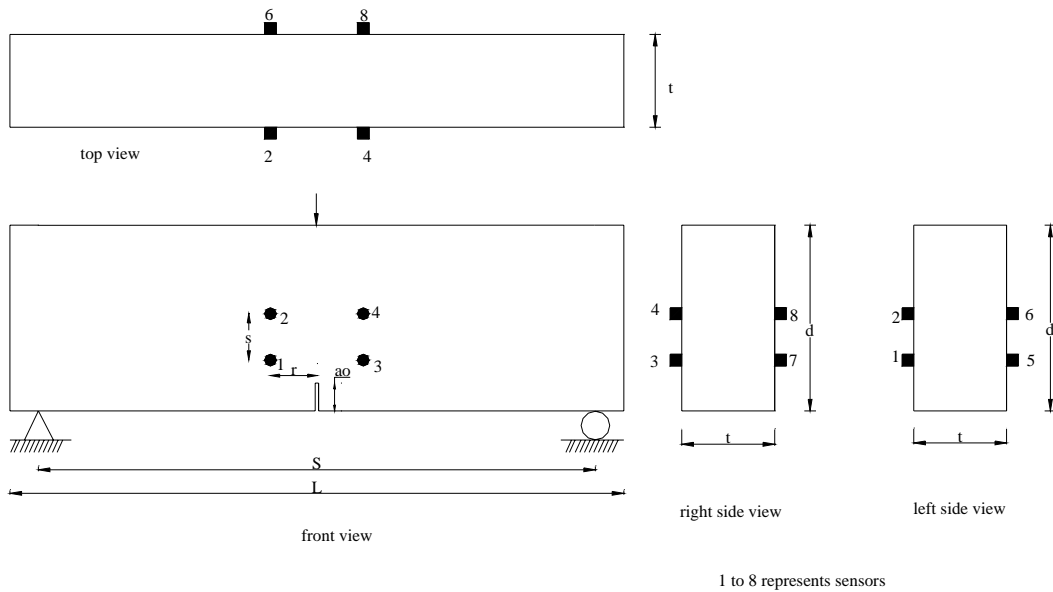

Figure 1a. Experimental set up of the three-point bend test with attached sensors.

The experimental setup consists of loading frame with data acquisition system, and an acoustic emission monitoring system. Material testing system of capacity 1200 kN was used as loading frame with data acquisition. The data acquisition records load, CMOD, midspan displacement, and time. The AE acquisition system records AE parameters. The AE system used in this present experimental study was a 8 channel AEwin[30] for SAMOS E2.0 (Sensor based Acoustic Multi channel Operating System) developed by Physical Acoustics Corporation (PAC). AE test set up consists of AE sensors (transducers), pre-amplifiers, processing instrumentation, and AE win

SAMOS software. The transducers used in the ex- perimental study were R6D resonant type AE differ-

d = depth of the beam, L = length of the beam, l = span of the beam and t = thickness of the beam

Figure 1b. Schematic diagram of the three point bend test specimen.

ential transducers. In general differential sensors are used in environments where very low level AE signals need to be processed and is also applicable in high noise environments. The output of a differential sensor is processed by a differential amplifier. By using a differential preamplifier, common mode noise is eliminated, resulting in a lower noise output from the preamplifier and a higher electrical noise rejection in difficult and noisy environments. The AE sensor diameter is 19mm and its height is 22.0mm and works in the temperature range of – 65^0C to 177^0C. The AE sensor has peak sensitivity at 75 dB with reference 1V/(m/s) [1V/mbar]. The operating frequency is 35kHz – 100kHz. An essential requirement in mounting a sensor is enough coupling between the sensor face and the concrete test specimen surface. Vacuum grease LR (high vacuum silicon grease) was used as couplant in the present experimental study. Before mounting the sensors on testing specimen, the sensor's surface was cleaned so that to make sure about allowing maximum couplant adhesion. Application of a couplant layer was thin, so that it could fill the gaps caused by surface roughness and eliminate air gaps to ensure good acoustic transmission. All the sensors were held firmly to the testing surface. The AE signals were amplified with a gain of 40 dB in a preamplifier. The threshold value 40 dB was selected to ensure a high signal to noise ratio. The specimens were tested under CMOD control at the rate of 0.0004mm/sec using MTS (Material Testing System) load frame.

The midspan downward displacement was measured using Linear Variable Displacement Transducer (LVDT) placed at center of the specimen under bottom of the beam. A clip gauge was used to measure the CMOD. AE signals over 40 dB were recorded as AE waves with classical AE parameters.

3.2 *Specimen preparation*

Details of the 9 specimens tested in this experimental study are given in Table 1. Notched plain concrete three-point bend specimens of different strengths are used in the experimental study. All specimens were cast with same batch of concrete in a specially made wooden moulds and compacted using a needle vibrator. Along with test specimens, cubes and cylinders were also cast for compressive strength determination. Table 2 shows concrete mix proportions used to prepare the test specimens. After casting the specimens demoulding was carried out with a time gap of 24 hours. The 28th day compressive strength of concrete mixes are 77.9 MPa, 63.7 MPa and 60.5 MPa. These were obtained as the average values from tests carried out on 5 cube samples (15 cm in width and 15 cm in height) after curing them for 28 days. Schematic diagram of the three-point bend test specimen is shown in Figure 1b. Three specimens of each type (total 9) were tested for measuring fracture energy, G_F. The maximum load was reached in about 5 minutes. A separate test was performed varying the sensor positions

Table 1. Details of the specimens tested

Concrete Mix	28th day compressive strength of cubes (MPa)	Notch details		Specimens tested	Sensors (Resonant type)	Threshold (dB)	Dimensions of the specimen (mm)				Sensors position from centre of the notch (mm)	
		Notch depth (a_0) (mm)	Notch/beam depth ratio (a_0/d)				Length (L)	Span (S)	Thickness (t)	Depth (d)	r	s
Mix-F	77.995	160	0.150	3	R6D	40					130	130
		160	0.150	3	R6D	40	1010	960	80	320	130	130
		160	0.150	3	R6D	40					130	130
Mix-E	63.714	160	0.150	3	R6D	40					130	130
		160	0.150	3	R6D	40	1010	960	80	320	130	130
		160	0.150	3	R6D	40					130	130
Mix-C	60.1	160	0.150	3	R6D	40					130	130
		160	0.150	3	R6D	40	1010	960	80	320	130	130
		160	0.150	3	R6D	40					130	130

Table 2. Concrete mix proportions

Property	Mix-F	Mix-E	Mix-C
Water/binder ratio	0.335	0.352	0.35
Cement, kg/m^3	450.0	450	440.0
Micro silica, kg/m^3	56.25	45.0	31.5
Fine aggregate, kg/m^3	706.95	704.0	437.1
Coarse aggregate, kg/m^3	1058.00	1028.35	1277.4
Water, kg/m^3	150.97	158.4	168.52
Superplasticiser, (% weight of cement content in mix)	1.2	1.2	1.2
Compressive strength, N/mm^2 (28-days)	77.995	63.714	60.1

along the span of the beam with respect to a fixed source of sound wave pulses at the left end of the beam. The amplitude variation as the sensor position is changed plotted in the Figure 1d. There is certainly attenuation experienced by the wave pulses. The amplitude reduction at the sensor position in our experiments can be obtained from the Figure 1c. The variation in the amplitude from the source can be determined from the equation (2).
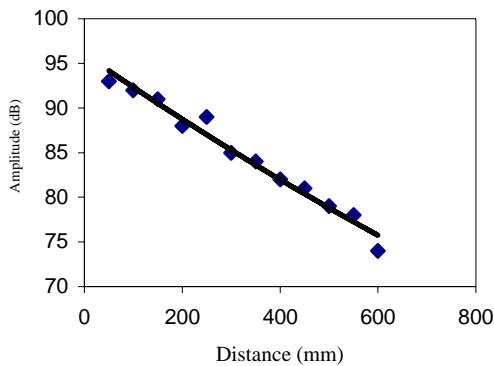
$$\text{Amplitude} = 95.807e^{-0.0004d} \qquad (2)$$

Where d is the distance from the source.

4 b-VALUE CALCULATION

To carry out b-value analysis the data recorded during the experiments were processed with a computer program developed. A computer program developed to carry out the b-value analysis. The data obtained from the experiment was used as input to this computer program developed by the authors. The b-value based on Gutenberg-Richter formula is calculated from the cumulative frequency-amplitude plots for incremental ranges of the monotonically applied loads. Table 1 shows the details of the specimens tested in this experimental study. Figure 2a shows a load versus time plot during test.
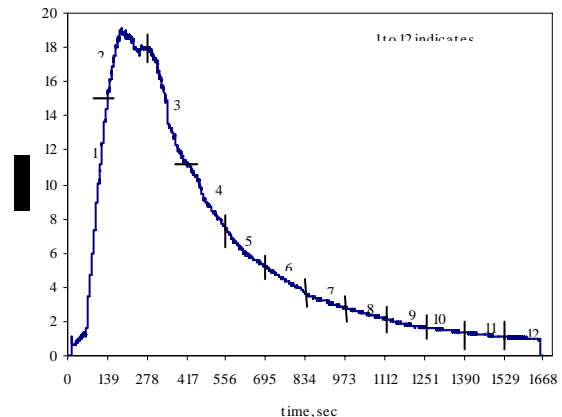

Figure. 1c. Attenuation experienced by the wave pulses.

Figure 2a. Load vs. time plot divided into 12 parts.

The *b*-value is the negative gradient of the log-linear slope of acoustic emission frequency-amplitude graph. The slope of this particular graph is *b*-value. Therefore the *b*-value represents the amplitude distribution. A typical plot of frequency versus amplitude graph is shown in Figure 2b and lease-squares curve fitting procedure was used to plot this graph.
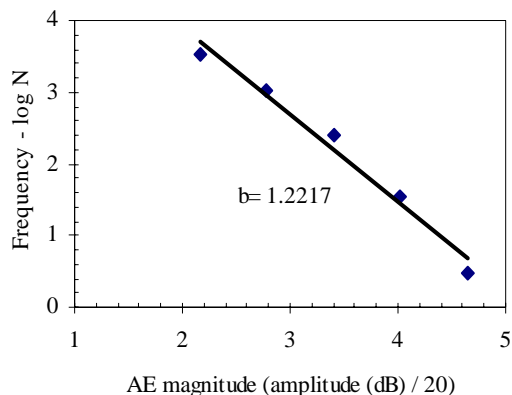

Figure 2b. A typical plot showing calculation of *b*-value.

Researcher found that equation (1) can be applied to AE data to calculate the *b*-value based on the AE data recorded during the tests[20-22]. However, AE amplitude data should be divided by 20 to get the same form of the equation (1). Because in equation (1) the earthquake magnitude *M* is defined in terms of logarithm of maximum amplitude but the AE peak amplitude is measured in dB[20-22]. Following Colombo[20] *et al* in this experimental study a procedure for obtaining the *b*-value has been adopted. In literature the investigators dealing with the study of concrete have tried to obtain the *b*-value from cyclic loading applied to the specimens[20]. From literature it was observed that previous investigators reported the *b*-value for each of the cycles[20]. However, in the present work the authors feel that it is not necessary to perform cyclic loading which is more tedious and time consuming. Instead in this present study the load-time diagram under monotonically loading and unloading is considered as one cycle as shown in Figure 2a and it can be divided into as many divisions (or parts) as possible. Figure 2c show *b*-value over time calculated by dividing the load versus time plot into 10 divisions (30553 events), 12 divisions (20369 events) and 8 divisions (24443 events). It is important to choose the number of events for calculation of b-value. In this present work the authors have chosen 12 such divisions. For entire calculation the load versus time graph was considered for 12 divisions and calculations were carried out. By choosing 12 divisions the ranges of AE amplitude from a threshold of 40 dB to a maximum 100 dB in steps of 5 dB was chosen. In each such divisions, namely 1,2,3,…. etc., the amplitude and the corresponding frequency of events are plotted in log scale.
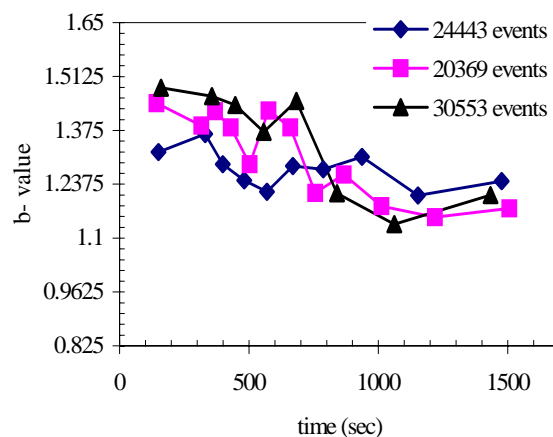

Figure 2c. Calculation of b-value for 5th part corresponding to Channel 2. The calculation for *b*-value was done for group of events.

The *b*-value thus obtained is plotted with respect to time as shown in Figure 2c. The *b*-value varies over time. And also it means that *b*-values vary with the various stages of fracture process of specimen. The intension is to fix the *b*-values broadly during pre-peak, peak and post-peak regions of load–deformation plot for various grades of concrete.

5 RESULTS AND DISCUSSION

Table 3 shows the values of fracture energy for all specimens tested in this experimental study. The *b*-values reported in Figure 2c show that the b-value decreases with time. It means that b-value progressively decreases with increase in damage level. While b-value is around 1.4 to start with it ends up at 1.2 at the end of the test. This is also depicted in the Figures 3a, 3b and 3c. Figure 4 and Figure 5 show frequency versus amplitude plots and corresponding b-values at various stages of fracture for Mix-E and Mix F respectively for channel 8 and the position of the same channel (sensor) was shown in Figure 1a. Figure 6 –Figure 7 show load-time, load-CMOD and load-deflection plots for test specimens made with Mix F and Mix-E respectively. Although nothing new could be said about these plots, it is interesting to see that they confirm the already known facts. Figure 8a and Figure 8b show the load versus time plots and load versus CMOD plots. From Figure 8a one can observe that as strength decreases the load carrying capacity also decreases and it is a well known fact and confirm the earlier results. Table 3 summarizes the various experimental observations.

The rate at which b-value decreases with deflection appears to be by and large same in all the three different mixes. It indicates that the decrease of b-value seems to be not influenced by the grade of concrete.

Table 3. Measured maximum loads, fracture energy and *b*-values at various positions of load –time plot.

Speci-men	Notch/depth a_0/d	Peak load P_{max} (N)	Work of fracture (N-m)	Fracture energy, N/m	Average fracture energy, (N/m)	b-value (Channel 8)			b- value (Channel 8)	
						Pre-peak	Peak	Post-peak	Mini-mum	Maxi-mum
Fln₁a	0.15	19316.385	2.5687	118.00						
Fln₁b	0.15	23646.961	2.7637	127.00	133.37	1.588	1.5406	1.1851	1.1063	1.588
Fln₁c	0.15	19131.463	3.3986	156.10						
Eln₁a	0.15	19135.11	3.8523	177.03						
Eln₁b	0.15	19131.75	3.1991	147.017	151.26	1.445	1.423	1.1756	1.1532	1.4449
Eln₁c	0.15	20692.77	2.8234	129.75						
Cln₁a	0.15	17777.20	2.9122	133.832						
Cln₁b	0.15	----	----	----	130.5	1.2968	1.3328	1.0699	1.0699	1.4317
Cln₁c	0.15	17327.34	2.7973	128.55						

In all the 3 mixes the *b*-value is about 1.4 at the peak load and decreases to a value 1.2 at the end of the test when the specimen has just collapsed. In all the tests the b-value is shown to occur just prior to the peak load and not earlier than that, apparently because events could not be recorded till about close to the peak load.
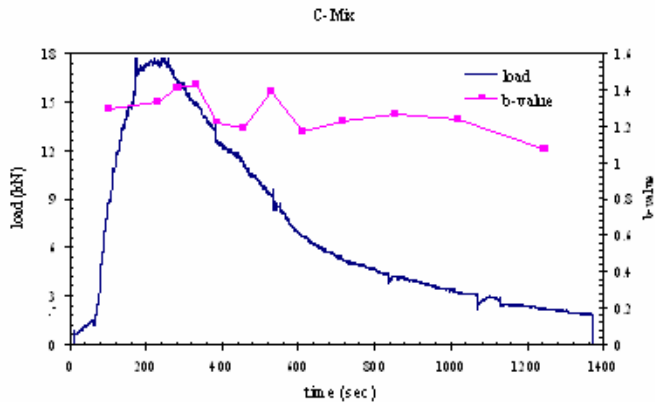

Figure 3a. Load-time and variation of b-value with respect to time for Mix-C (channel 8).

The high value of b just before the peak load indicates occurrence due to microcracking activity only ahead of the crack tip. A high value of b results from large number of events with corresponding small amplitudes. Soon after microcracking, as they coalesce to form a single macrocrack, obviously the number of events will be less with corresponding large amplitudes, thus leading to a lower b-value. In fact, further extending the usefulness of the b-value, it could be said that b-value near the peak load indicative of microcracking can really help to understand the magnitude of microcracking. Larger the microcracking which is also dependent on process
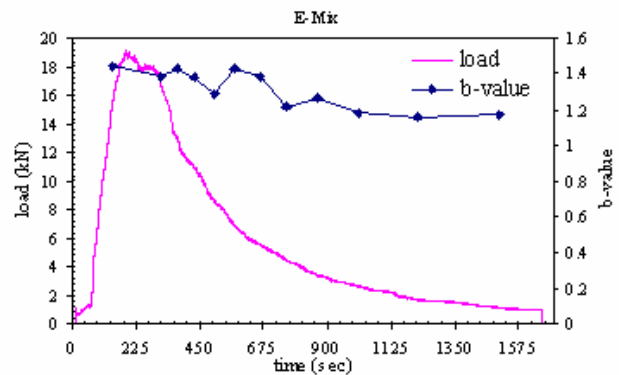

Figure 3b. Load-time and variation of *b*-value with respect to time for Mix-E (channel 8).
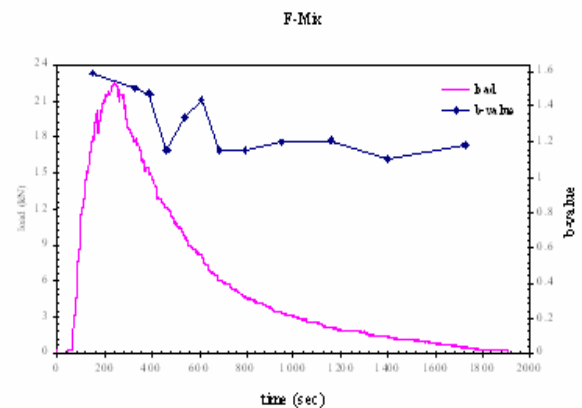

Figure 3c. Load-time and variation of *b*-value with respect to time for Mix-F (channel 8).

zone size, larger will be the b-value. Further tests are planned to relate the process zone size with the b-value. Nevertheless the b-value at the end of the test near the collapse load which is indicative of one single macrocrack will remain the same because irrespective of any process zone size at the collapse state there will be only one single crack.
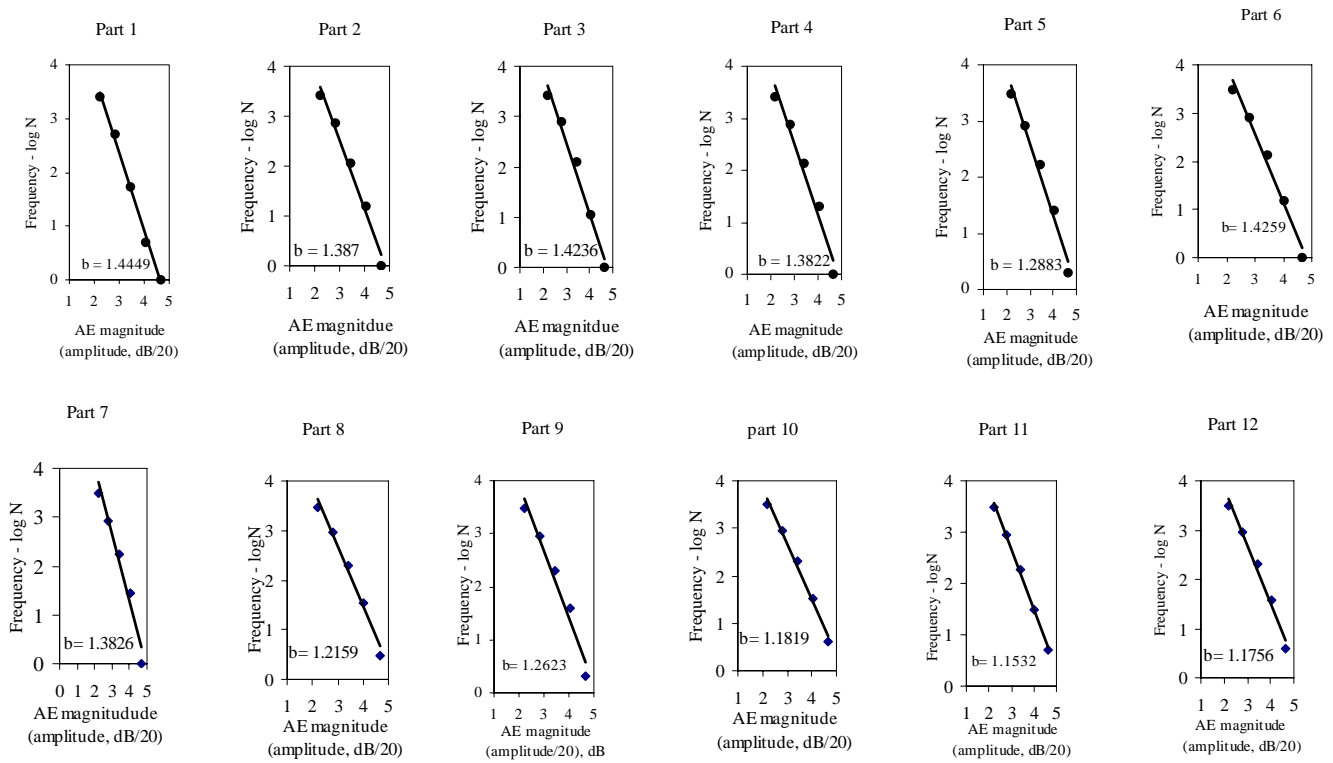
Figure 4. Frequency versus amplitude plots and corresponding *b*-values during 12 divisions for channel 8 for Mix-E (Specimen ELN₁a).
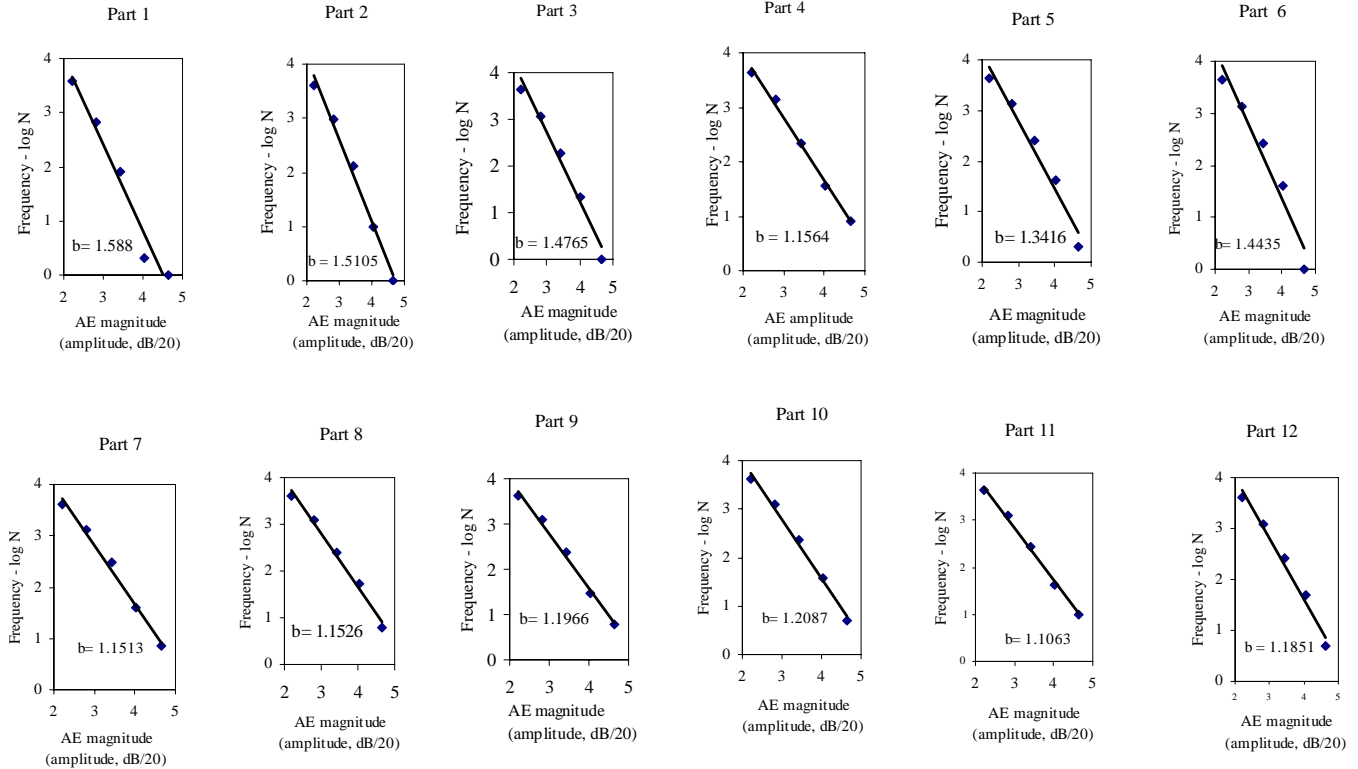

Figure 5. Frequency versus amplitude plots and corresponding *b*-values during 12 divisions for channel 8 for Mix-F (Specimen FLN₁b)
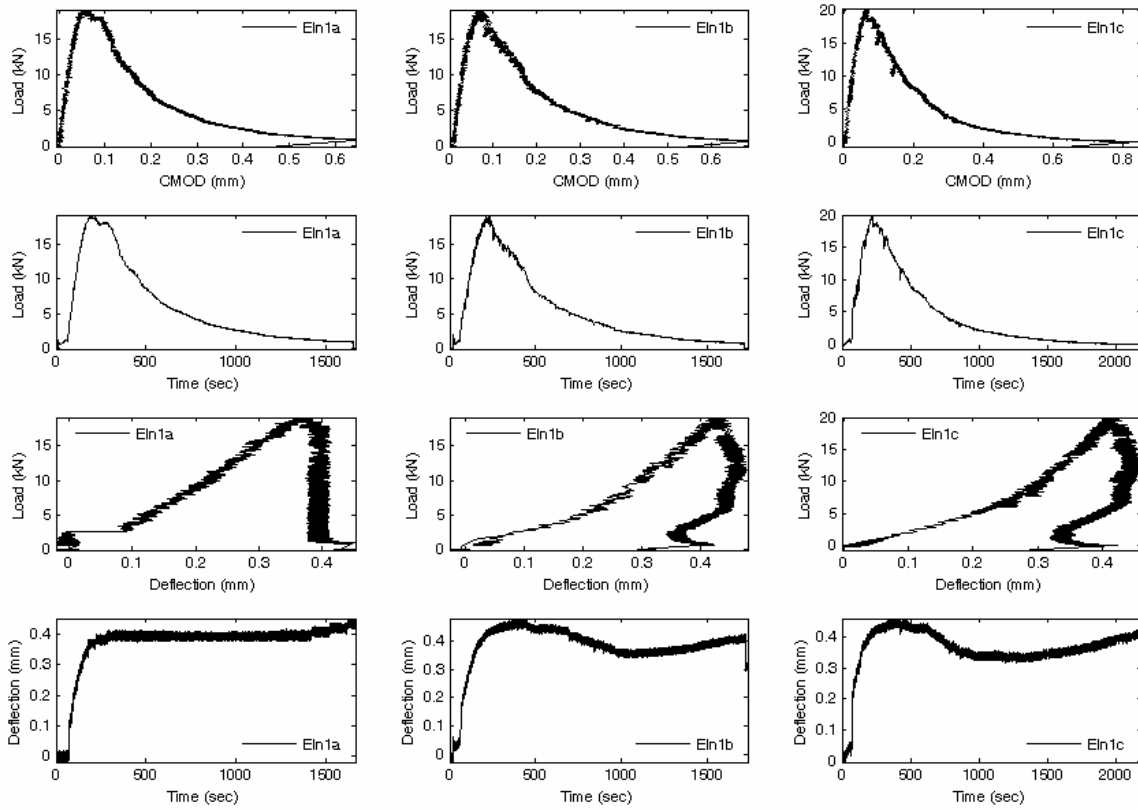
Figure 6. Load versus CMOD, Load versus Time, Load versus Deflection and Deflection versus Time for E-Mix, (notch/depth ratio=0.15).
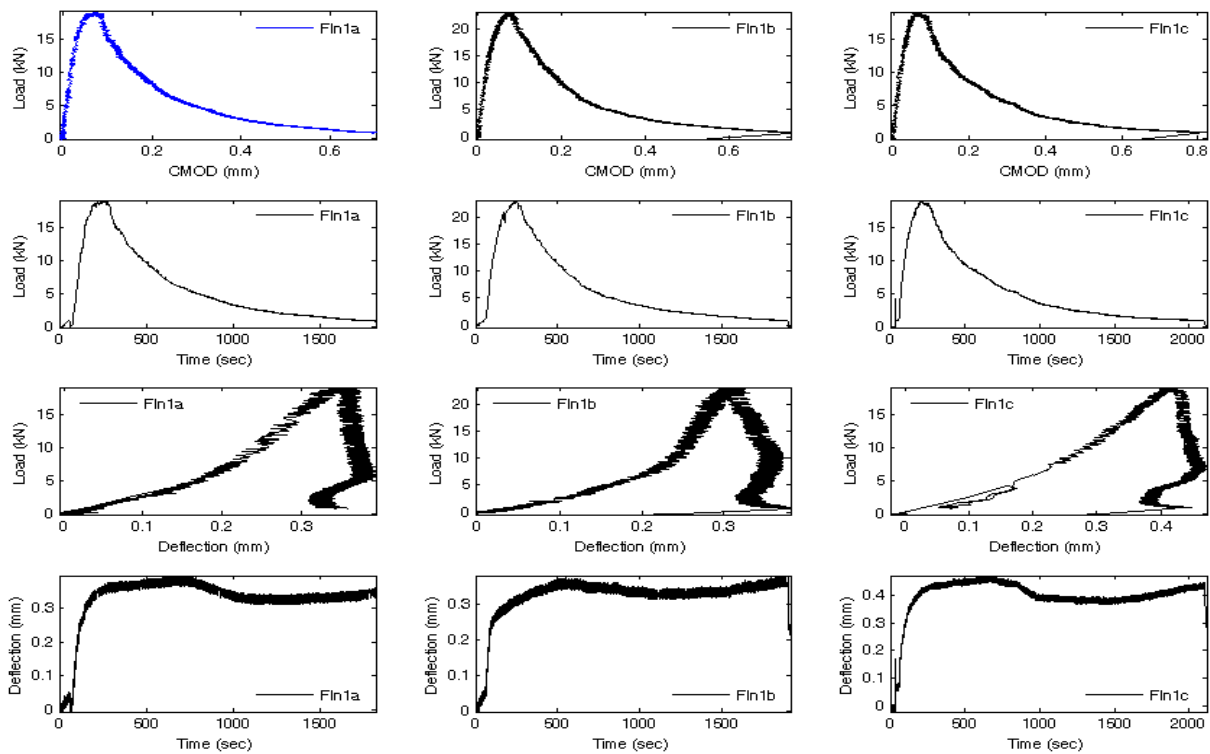

Figure 7. Load versus CMOD, Load versus Time, Load versus Deflection and Deflection versus Time for F-Mix, (notch/depth ratio=0.15).
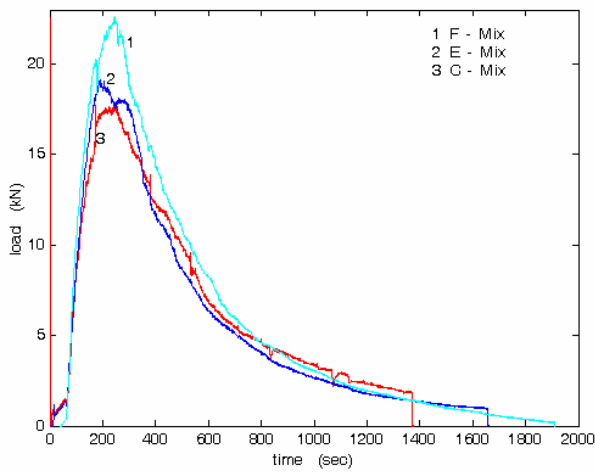
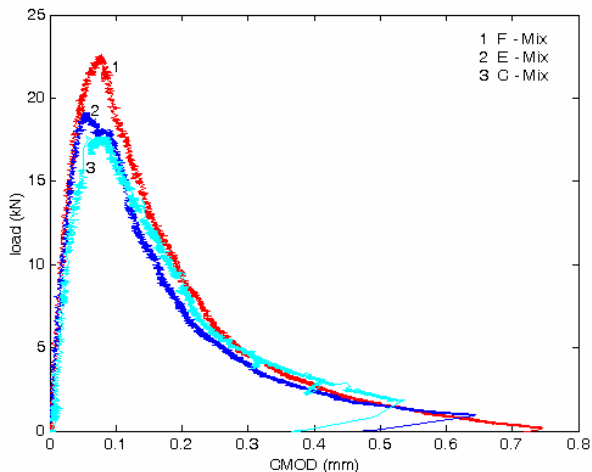Figure 8a. Variations of load with respect to time for mixes C, E, and F

Figure 8b. Variations of crack mouth opening displacement (CMOD) with respect to load for mixes C, E, and F

6 CONCLUSIONS

In this investigation an attempt is made to obtain the influence of damage on *b-value.* While all earlier investigations focused on *b*-value variation in cyclic loading of RC beams to the best of the author's knowledge there is no work attempting to relate *b*-value to the level of damage in plain concrete beam. A clear demarcation of macro and micro cracks can be possible only in plain concrete beams and not in reinforced concrete beams. The present work has enabled to conclude the following:

1   The *b*-value begins to appear only near about the peak load, just before it.
2   The *b*-value decreases from the peak load till the load becomes zero ending up at a value of about 1.2.
3   The *b*-value is not significantly influenced by the grade of concrete

Therefore it may be further said that in damage detection of concrete structure, a value of *b* close to 1.2 might be indicative of complete local distress of the concrete there. Ofcourse, a fact still to be understood is how to locate that point where distress has occurred. If the value is about 1.4 and higher, the concrete there is still intact. Further work is planned to quantify the findings in further detail.

REFERENCES

Van Mier, J G.M. Fracture process of concrete, Assessment of Material Parameters for Fracture Models, CRC press, 1997.

Bazant, Z. P., Fracture and size effect in concrete and other quasi-brittle materials CRC press, 1998.

Karihaloo, B.L., Fracture mechanics and structural concrete. New York: Longman Scientific & Technical, 1995.

Shah, S.P., Swartz, S.E., Ouyang, C., Fracture mechanics of concrete: Applications of fracture mechanics to concrete, rock and other quasi-brittle materials, John Wiley & Sons, Inc, New York; 1995.

Ronnie K. Miller, Paul McIntire. Non-destructive Testing Handbook, Vol. 5, Acoustic Emission Testing, American Society For Non-destructive Testing INC; 1987.

Chang Perter, C., and Liu Chi S. , Recent research in non destructive evaluation of civil engineering structures. J Mater in civil Eng ASCE., 2003, pp. 298-304.

Ohtsu M., A review of acoustic emission in civil engineering with emphasis on concrete. J Acou Emis.,Vol. **8**, 1989, pp.93-98.

Adrian A. Pollock, Acoustic emission inspection, Technical report, TR-103-96-12/89., Physical Acoustics corporation., 195 Clarksville Road, Primceton Jct., NJ., USA.

Maji, A., and Shah, S.P., Process zone and acoustic-emission measurements in concrete, Exp Mech. 1998, March, pp.27-34.

Uomoto Taketo, Application of acoustic emission to the filed of concrete engineering, J Acou Emis,Vol. 6, 1987, pp.137-144.

Ohtsu, M., The history and development of acoustic emission in concrete engineering. Mag of Conc Res., Vol.48**,** 1996, pp**.**321-330.

Rossi, P., Rober, J. L., Gervais J P., and Bruha D., The use of acoustic emission in fracture mechanics applied to concrete., Eng Frac Mech,Vol. 35**,** 1990, pp.751-763.

Richter Charles F., Elementary Seismology, W.H Freeman and company San Fracisco and London, (1958).

Gutenberg, B. and Richter, C.F., In Siesmicity of the Earth and Associated Phenomena. Princeton University Press. Princeton, NJ., USA, 1954, 2nd edn.

Mogi, K., Magnitude-frequency relation for elastic shocks accompanying fracture of various materials and some related problems in earthquakes. Bull. Earthquake. Res. Inst., Tokyo Univ., Vol. 43,1965, pp.237-239.

Kramer, L. Steven., Geotechnical earthquake engineering., 2004. pp.121-125.

Mogi, K., Earthquakes and fractures, Tectonophysics, Vol.5**,** 1967, pp.35-55.

Scholz, C. H., The mechanics of Earthquakes and Faulting - 2nd Edition, Cambridge University Press, 2002, pp. 224-228.

Shearer, P.M., Introduction to Seismology, Cambridge University, 1999, England, 1-189.

Colombo, I.S., Main, I.G., and Forde, M.C., Assessing damage of reinforced concrete beam using "b-value analysis of Acoustic emission signals. J mater civil eng, ASCE , 2003, pp. 280-286

Cox, S. J. D., Meridith, P. G., Microcracking formation and material softening in rock measured by monitoring acoustic emissions. International Journal of Rock Mechanics and

Mining Science & Geomechanics Abstracts ,Vol.30, 1993, pp.11-24.

Rao, M.V. M.S., Significance of AE-based b-value in the study of progressive failure of brittle rock: Some examples from recent experiments. 14th WCNDT, December 8-13; 1996, New Delhi, India., pp. 2463-2467.

Shiotani, T., Ohtsu, M. and Ikeda, K. Detection and Evaluation of AE Waves due to Rock Deformation. J Constr and Build Mat., Vol.15, 2001, pp.235-246.

Lockner, D., The role of acoustic emission in the study of rock fracture. Int J Rock Mechanics and Mining Science & Geomechanics Abstracts, Vol.30, 1993, pp.883-899.

Rao, M.V.M.S., Prasanna Lakshmi, K. J., Analysis of b- value and improved b-value of acoustic emissions accompanying rock fracture. Curr Sci. Vol. 89, 2005, pp.1577-1582.

Sammonds, P.R., Meridith, P.G., Murrel, S.A.F., and Main, I.G., Modelling the damage evolution in rock containing pore fluid by acoustic emission. Eurock '94, Balkema, Rotterdam, The Netherlands.

Carpinteri A., Lacidogna G., Damage diagnostic in concrete and masonry structures by acoustic emission technique, Facta universities., Series: Mechanics, Automatic Control and Robotics, Vol.3, 2003 pp.55-764.

Main, I.G., P.G. Meredith and C. Jones, A reinterpretation of the precursory seismic b-value anomaly from fracture mechanics, Geophysics Jour(1989), pp.31-138.

Shiotani T and., Yuyama S., Li Z.W., and Ohtsu M., Quantitative evaluation of fracture process in concrete by the use of improved b-value. 5th Int. symp. non-dest. test. in civil engg. (ed. Uohoto T.) , Elsevier science, Amsterdam, 2000, pp. 293-302.

Physical Acoustic Corporation (PAC), SAMOS AE system User's manual Rev.2 May (2005).

RILEM Committee 50-FMC draft recommendations Determination of the fracture energy of mortar and concrete by means of three-point bend tests on notched beams., Mater and struct,Vol.18, 1985, pp.285-290.